Proc. of 2nd KSV Conference
POSTECH, Pohang, Korea, Nov. 14, 2003

Visualization of the two-layered electroosmotic flow and its EHD instability in T-channels by micro PIV

Kwan Hyoung Kang,* Sang Min Shin,† Sang Joon Lee,* and In Seok Kang†

Abstract

An interfacial instability has recently been observed for the DC- and AC-powered electroosmotic flows of the two miscible electrolyte layers having different concentrations in microchannels. It is rather contrary to our common belief that the flow inside a microchannel is generally stable due to the dominant role of the viscous damping. In this work, we visualized the electroosmotic flow inside a T-channel to validate the numerical predictions. It is clearly shown that the strong vortices (which characterize the interface shapes) are generated at the interface of the two fluids, as was predicted in the numerical analysis.

Key Words : Electroosmotic flow (전기 삼투 유동), Flow instability (유동 불안정성), Electrohydrodynamic (EHD) flow (전기 유동), Micro PIV (마이크로 입자 영상 유속계)

1. Introduction

In a microfluidic condition, the flow is usually very stable due to the dominant role of viscous damping, and consequently, mixing liquids is actually like trying to stir molasses into honey [1]. The laminar flow and subsequent diffusive mixing character often necessitate passive or active mixing devices. On the contrary, such a high stability and low mixing character can be beneficially utilized (in the case of the two parallel streams) for membraneless micro fuel cell [2,3] and measurement of diffusive character of small molecules [4].

The flow instability observed in a microfluidic condition by Chen and Santiago [5] is really interesting, considering such a general nature of the flow in the microscale dimensions. According to their observation, the two parallel electrolyte streams in a T-channel driven by a DC electroosmotic flow shows very fast growth of interfacial waves such as shown in Fig. 1. Similar but rather complex features have been observed for the AC case by Shin et al. [6]. Such kind of flow instability occurs only when the concentrations of the solution is different.

This kind of rather violent flow instability is certainly extraordinary in the microfluidic flows. It draws much attention since it has a potential to be beneficially utilized as a means to promote mixing in microfluidic systems. For instance, we can artificially make the concentration of two streams different by adding small amount of salt to one of the streams, in anticipation of such a flow instability and subsequent rapid mixing. Conversely, such instability will be a potential trouble in microfluidic devices requiring stable transport of species.

Kang et al. [7] has recently showed numerically that the instability is originated from the concentration gradient. They predicted that strong vortices are generated due to the body force acting on free charges (see Fig. 2b and Fig. 9 for a magnified view). The vortices induce the peculiar interface pattern such as shown in Fig. 1. An experiment is undergoing to verify the numerical results. In this paper, the preliminary results of the experiment are presented.

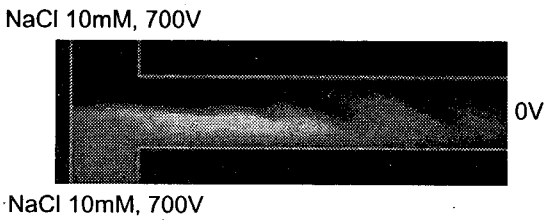

Fig. 1 Interfacial instability of the electroosmotically-driven two-layered flow of different concentrations.

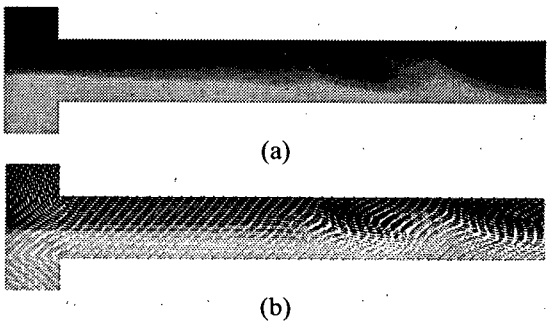

Fig. 2 Results of the numerical simulation: (a) concentration distribution; (b) flow field (see also Fig. 9).

* Dept. of Mech. Eng., Pohang Univ. Sci. & Tech.
E-mail: khkang@postech.edu. (Dr. Kwan Hyoung Kang)
† Dept. of Chem. Eng., Pohang Univ. Sci. & Tech.

2. Experiment

Fabrication of the glass chip. The standard photolithography techniques and the wet-etching process are used for the T-channel fabrication. The 200nm poly-silicon layer is deposited onto the glass substrate as a sacrificial etch mask in hydrofluoric acid. The positive photoresist (AZ 4620, Clariant) and the reactive ion etching equipment are used to pattern T-channel. The deprotected glass areas were etched isotropically in the 50% hydrofluoric acid solution followed by removal of the polysilicon layer. The basic layout of channel width is 50μm and the channel is etched to a depth about 50μm. The sand blasting method is used to make the 1mm diameter hole on the glass wafer. The glass wafer which is patterned with a T-channel is sealed by a thermal bonding with a second pyrex glass wafer. The reservoirs were connected to the glass hole with epoxy. Electrical contact with the solution is made by placing a platinum wire into the reservoir (see ref. [6] for details).

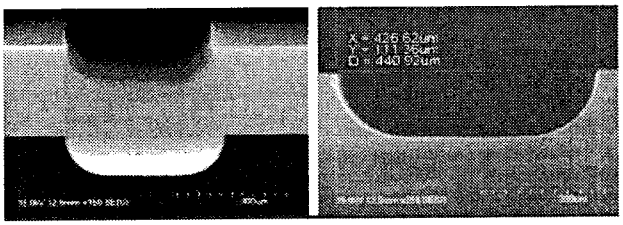

Fig. 3 SEM image of the etched glass

Fluorescence imaging. An inverted epifluorescent microscope (Nikon TE300) and a 100W mercury lamp were adopted to observe the fluorescence images of the flow. The fluorescent filter (Nikon B-2A) spectrally filtered at the peak fluorescence absorption and emission wavelengths of 450~490nm and 520nm. Images are captured by 12-bit CCD camera (Quantix 57, Photometrics) with a 530×526 imaging array of 13μm square pixel. The expose time of CCD camera is 2ms. Pixels are binned 2×2 to increase frame rate. The fluorescence images are analyzed by image analysis software (MetaMorph 6.1, Universal Image) (see ref. [6] for details).

Micro PIV system. The micro PIV system used in this work is schematically described in Fig. 4. A cooled CCD camera is used to capture images. It has the spatial resolution of 1024×1280 pixels and the dynamic range of 12bit. For the visualization of particle streaks, the halogen light is illuminated at the region of interest. For the PIV measurement of flow field, a two-head Nd:Yag laser is used. The location of image plane is changed by controlling the location of the focal plane of the camera. As the seeding particle, a fluorescent particle having the mean diameter of 1μm is used. A pair of consecutive images is obtained. The time delay between the two images is typically 1μsec.

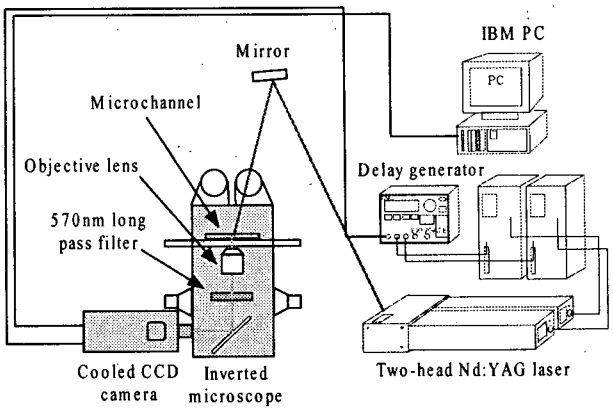

Fig. 4 Schematic diagram of micro PIV system and experimental apparatus

3. Experimental results

Figure 5 shows the streak lines of the seeding particles. Throughout the experiment, 1mM (upper stream) and 10mM (lower stream) of NaCl solution are used. For the T-channel shown in Fig. 5, the instability begins to occur above 2.7kV. Before the onset of instability (the case of Fig. 5a), a stable laminar flow is observed. The electroosmotic velocity is about 1.8 times greater at the upper branch of the channel. This is because the zeta potential is greater for the case of 1mM solution [6].

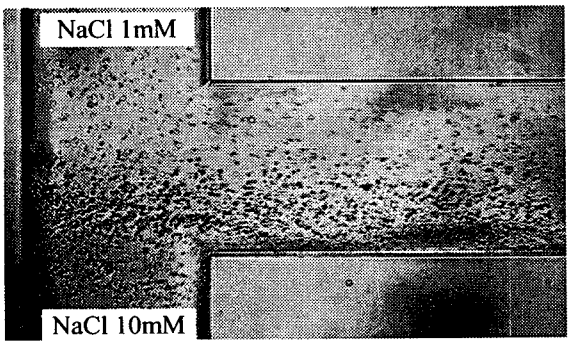

(a)

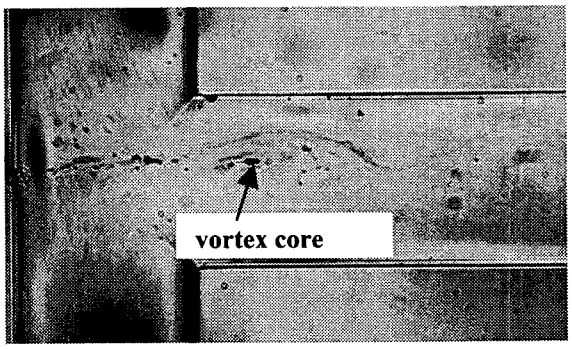

(b)

Fig. 5 Visualized particle streaks: (a) 300V; (b) 3kV.

After onset of instability, vortical flow pattern can be observed. A typical vortical flow pattern is shown in Fig 5b for the case of 3kV.

Figure 6 shows the PIV data for the different voltages. In the experiment, the amount of seeding particles was rather insufficient. So, we could not obtain enough velocity vectors. Nevertheless, a vortex structure is clearly shown in Fig. 6d. The vortices are in fact generated periodically and are convected by flow. Note that the condition of Fig. 6d corresponds to that of Fig. 5b.

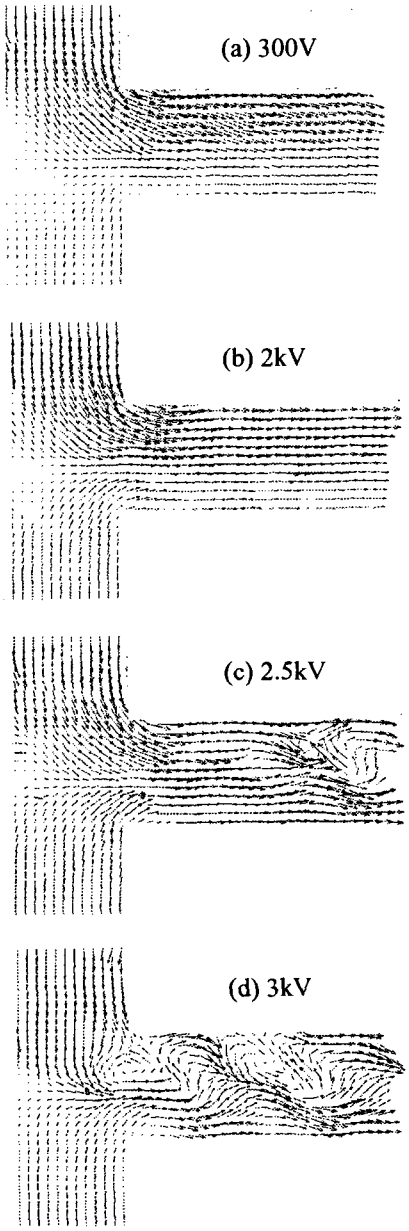

Fig. 6 PIV data

4. Discussions

In this section, we briefly discuss the origin of the free charges which is the key of the occurrence of the instability of the present investigation. As shown in Fig. 1, the overall shape of interface resembles that of the shear-induced interfacial waves such as the Kelvin–Helmholtz waves [8]. Actually, the osmotic slip velocity at the upper wall (at the converging channel) is a little greater than at the lower wall due to high zeta potential at the upper wall. The Reynolds number is, however, still too small compared to conventional criteria for the onset of the shear-induced instability. Most of all, the wave crests are rippled to the backward direction at the upper region of the channel. This is contrary to the case of the shear-induced instability, which decisively discourages to pursue the hydrodynamic origin of the instability.

What must be considered to the next will the electrohydrodynamic (EHD) flow and its stability. According to Landau and Lifshitz, the electric force density on bulk fluid ($\mathbf{f}_e$) can be written in isothermal conditions as [9]

$$\mathbf{f}_e = \rho_e \mathbf{E} - \frac{1}{2}\mathbf{E}\cdot\mathbf{E}\nabla\varepsilon$$

where ρ_e is the charge density, $\mathbf{E}$ is the electric field, ε is the electric permittivity. The EHD flow thus can be generated by the effects of induced charge ($\rho_e\mathbf{E}$-force) and dielectric constant variation ($\nabla\varepsilon$-force).

In the present case, however, the electrical permittivities of the fluid may be uniform over the entire domain. Therefore, for the generation of the EHD flow, the free charges must be induced in the domain. The free charges can be generated in two ways. First, the free charge can be generated when the electric field is applied to the region of conductivity (concentration) gradient, as schematically described in Fig. 7 (see ref. [7] for details concerning the polarization mechanism).

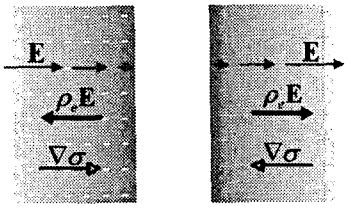

(a) (b)

Fig. 7 Polarization due to conductivity gradient. σ and the darkness level indicate the electrolyte concentration.

Second, the free charges can be generated by the difference in diffusivity of ions. As schematically shown in Fig. 8, the difference in diffusivity causes the non-uniform distribution of ions. The electrostatic potential generated by this kind of free charges is called the liquid junction potential [3]. It is shown, however, that the magnitude of this kind of free charges is very small, for the present problem of consideration, compared to that generated by the former mechanism [7].

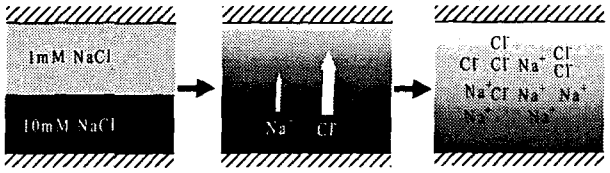

Fig. 8 Polarization due to diffusivity difference. The darkness level indicates the electrolyte concentration.

5. Concluding remarks

The existence of the strong vortical flow pattern predicted by Kang et al. [7] is confirmed. It is in general difficult to generate vortical flow for the creeping flow. This kind of vortex-generation mechanism may be utilized as a simple means to enhance the mixing of heterogeneous fluids. The effectiveness in mixing enhancement should be investigated in the future work.

Acknowledgements

The present investigation was supported by the Brain Korea 21 Program in 2002 and by the POSCO Technology Development Fund in 2002 (Contract No. 1UD02013). I.S.K. was also supported by a grant from the Korea Science and Engineering Foundation (KOSEF) (Contract No. R01-2001-00410). We deeply appreciate the help of Mr. Guk Bae Kim and Mr. Chang Sub Yeo for the micro PIV experiment, and of Mr. Jae Wan Park for the numerical analysis.

References

1) J. Knight, 2002, "Honey, I shrunk the lab," *Nature* 418, 474.
2) R. Ferrigno, A. D. Strook, T. D. Clark, M. Mayer, G. M. Whitesides, *J. Am. Chem. Soc.* 124, 12930.
3) K. H. Kang and I. S. Kang, 2003, "Theoretical investigation on the liquid junction potential in a slit-like microchannel," *J. Electroanal. Chem.* (In press).
4) A. Hatch et al., 2001, "A rapid diffusion immunoassay in a T-sensor," *Nature Biotechnology* 19, 461.
5) C. H. Chen and J. G. Santiago, 2002, "Electrokinetic flow instability in high concentration gradient microflows," *Proc. 2002 Int'l Mech. Eng. Cong. and Exp.*, New Orleans, LA, CD vol.1, Paper No. 33563.
6) S. M. Shin, I. S. Kang, Y.-K. Cho, and G. Im, 2003, "Instability of electroosmotic flow under time-periodic electric fields," *Anal. Chem.* (Submitted).
7) K. H. Kang, J. W. Park, I. S. Kang, and K. Y. Huh, 2003, "Electrohydrodynamic instability of two-layered miscible fluids with different concentrations in microchannels," *Phys. Rev. E.* (Submitted).
8) Van Dyke, 1982, *An Album of Fluid Motion*, The Parabolic Press, Stanford, California.
9) L. D. Landau, and E. M. Lifshitz, 1960, *Electrodynamics of Continuous Media*, Pergamon Press, Sydney.

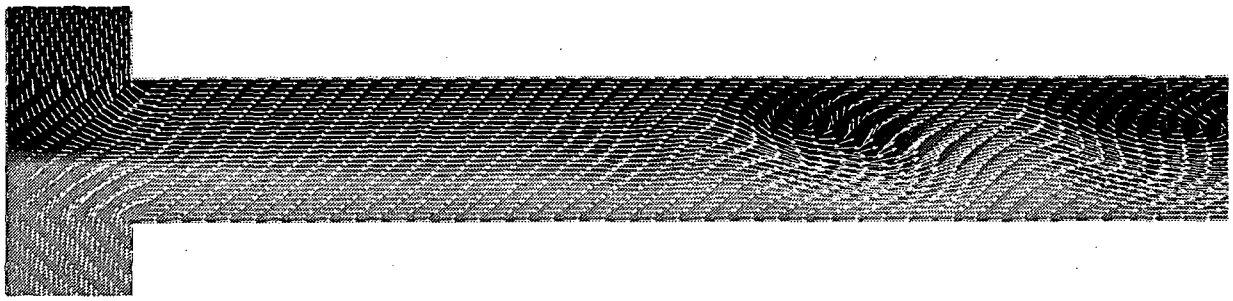

Fig. 9